Advanced monitoring system applied to Colle Isarco viaduct

Carlo CAPPELLO[1], Angela BELTEMPO[1], Alessio BONELLI[1],
Carlo COSTA[2], Denise BOLOGNANI[1], Oreste Salvatore BURSI[1], Daniele ZONTA[1,3]

[1] Dept. of Civil, Environmental and Mechanical Engineering, University of Trento, via Mesiano 77, 38123 Trento, ITALY carlo.cappello@unitn.it, angela.beltempo@unitn.it, alessio.bonelli@unitn.it, denise.bolognani@unitn.it, oreste.bursi@unitn.it
[2] Autostrada del Brennero SpA, via Berlino 10, 38121 Trento, ITALY direzione.tecnica.generale@autobrennero.it
[3] Dept. of Civil and Environmental Engineering, University of Strathclyde, 75 Montrose Street, Glasgow, G11XJ, UK daniele.zonta@strath.ac.uk

Key words: bridge retrofit, post-tensioning, creep, B3 model, structural health monitoring, topographic stations, fiber optic sensors.

Abstract

With its 13 spans and total length of 1028 m, Colle Isarco Viaduct is among the longest bridges in the Alpine region and is a link of strategic importance on the highway corridor connecting Northern Italy to Austria. The bridge was designed and built between 1968 and 1971 and underwent repair interventions in 19*88, 1999 and 2007. To cope with today's* growing traffic load demand, the bridge was recently further retrofitted through installation of an external post-tensioning system. The effectiveness of this work, completed in 2015, is currently being assessed through extensive structural health monitoring. In this note, we illustrate the bridge, its history and the past maintenance works. We describe in detail the rationale behind the design of the new monitoring system and how the data acquired shed light on the observed past behavior of the bridge and on the effectiveness of the new retrofit intervention.

1 INTRODUCTION

The Colle Isarco Viaduct is a link of strategic importance on the highway corridor connecting Northern Italy to Germany. Overall, the viaduct consists of two structurally independent decks, supporting the two 10.30 m wide highway carriageways, northbound and southbound, each of a total length of 1028 m covering 13 spans. The main span of the viaduct, the longest in the region, is 163 m long, and is spanned with two symmetric balanced segmental reinforced concrete cantilevers, supporting a suspended span (Fig. 1). The bridge was opened to traffic in 1971. In the following years, the main span experienced progressive abnormal deflection, exceeding 200 mm in 1984. This unexpected behavior prompted the owner, Autostrada del Brennero SpA, to undertake a drastic retrofit in 1988. The highway administration undertook a new retrofit between 2014 and 2015, with the aim of enhancing the bridge's load carrying capacity through external posttensioning. This intervention was accompanied by extensive structural health monitoring (SHM) [1,2], seeking to assess the effectiveness of the work, provide information allowing better assessment of future structural performance [3–6] and support decisions [7–9]. Since summer 2014, the bridge deflection

has been continuously monitored with a topographic network and, starting in 2016, the main spans of the viaduct will be further instrumented with fiber optic sensors [10,11] and PT100 temperature sensors [12,13]. In the following, we first provide a description of the main span of the bridge, its history and maintenance works. Next, we illustrate in detail how the bridge behavior is interpreted using a finite element model. We then discuss the criteria applied to the design of the monitoring system, and we show some preliminary results.

2 CONSTRUCTION AND RETROFIT OF THE MAIN SPAN

The main span of the bridge is crossed with two symmetric balanced segmental reinforced concrete cantilevers, supporting a 45 m long suspended span (Fig. 2). Each cantilever arm juts 59 m out of the piers, and is counterbalanced by a back arm 91 m long. Overall, a cantilever contains 33 box-girder cast-in-place segments of depths varying from 10.80 m, at the pier, to 2.55 m, at the edge. The thickness of the top slab is constant and equal to 260 mm, while the bottom slab varies from 980 mm to 150 mm. A concrete of nominal class corresponding to modern Eurocode C35/45 was used for all cast-in-place elements of piers and girders. The prestress was applied by 32 mm diameter Dywidag ST 85/105 threaded bars, with 1030 MPa nominal tensile strength and initial jacking tension of 720 MPa. For each cantilever, the longitudinal force above the pier was around 120 MN and was provided by a total number of 266 tendons.

The viaduct was erected between 1968 and 1971; a detailed account of the construction can be found in [14]. Just after two years from the opening of the bridge, the monitoring data started exhibiting an abnormal progressive deflection drift: Fig. 3 shows, for example, the deflection recorded at the edge of the northernmost cantilever of the southbound carriageway. As opposed to a design prediction of less than 20 mm, the actual deflection reached 200 mm in 1984, with an apparent velocity of over 8 mm/year.

Figure 1: Main span of Colle Isarco Viaduct; left pier is #8, right is #9.

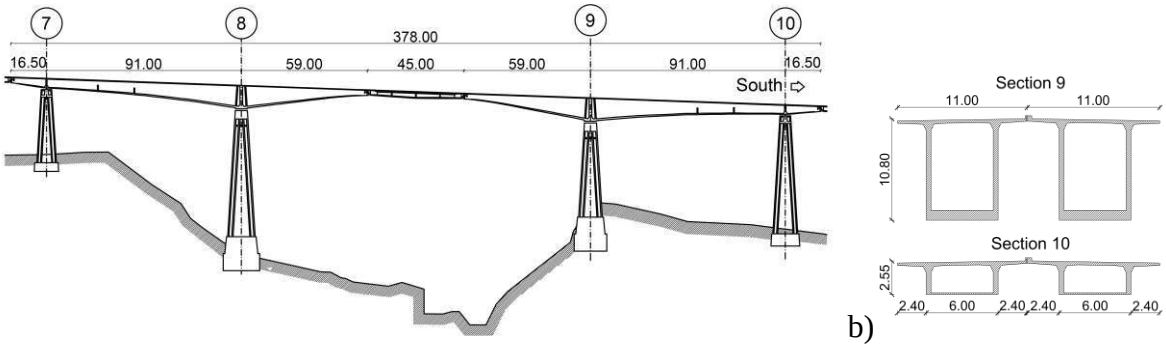

a) b)

Figure 2: Elevation of Colle Isarco main span (a) and cross-sections at piers #9 and #10 (b); dimensions in [m].

These observations prompted the owner to undertake, between 1988 and 1989, a radical retrofit of the main span in an attempt to prevent further deflection of the bridge. The rationale of the retrofit was to reduce the load on the main span by removing the original pavement over the cantilever arms and the suspended span, and replacing it with a thinner layer of lightweight asphalt. The effect of this work is evident in an immediate 70 mm recovery of the deflection, and in the disappearance of the deflection drift in the following years, as seen in Fig. 3. In the following years, dumpy level measurements showed the deflection drift had resumed at an apparent rate of over 2 mm/year.

In the end, the owner decided to retrofit the existing structure, and enhance its load-carrying capacity, by installing an external post-tensioning system. The retrofit was designed by the Autostrada del Brennero SpA technical office in collaboration with an engineering consultant, SEICO SRL, and carried out between 2014 and 2015. Details of the retrofit work are found in the relevant design documentation [15]. The additional prestress was provided by a total number of 212 0.6” diameter compact strands, with a jacking load of 213 kN. The additional longitudinal force produced above the pier was around 45 MN, which is almost 40% of the original prestress. To compensate for the additional post-tensioning force, the thickness of the box-girder top slab was increased from 260 mm to 285 mm before prestressing. Additional minor maintenance works were carried out along with the post-tensioning.

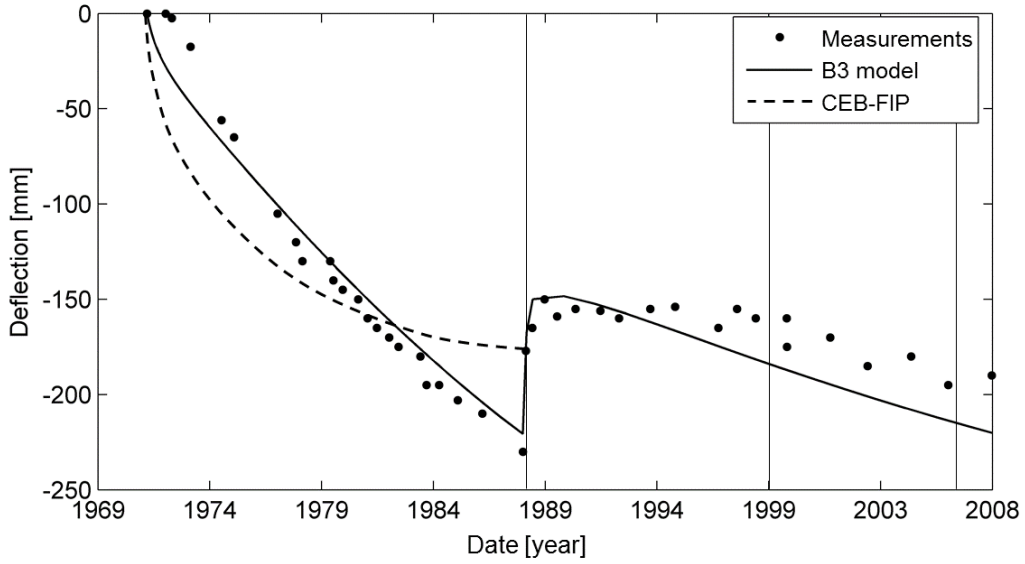

Figure 3: Deflection observed at the edge of the northernmost cantilever of the southbound carriageway. The experimental data are compared with the best fit achieved assuming CEB-FIP [16] and Bazant B3 [17] creep models.

3 BRIDGE MODELLING

All the analyses conducted in the past failed to provide a convincing explanation for the actual mechanical cause of such an abnormal deflection. Any attempt to explain the past behavior of the bridge using the classical CEB-FIP creep and shrinkage models [16], those currently recognized by Eurocode 2, appears unconvincing. We can clearly observe the discrepancy between observations and model in Fig. 3: the dashed line is the deflection predicted using a beam-like model of the cantilever that implements the Eurocode 2 creep model, with a choice of parameters that optimizes the fit with experimental observations.

Some papers recently published by Bazant [17] offer a more credible explanation for the apparently abnormal behavior of Colle Isarco viaduct. Bazant et al. [17] discuss the excessive deflection observed in a number large segmentally erected box girders, indirectly suggesting that Colle Isarco's behavior is typically observed in similar construction types. Bazant et al. [17] also note that classical CEB-FIP shrinkage and creep models are clearly unsuited to reproducing the long-term behavior of this class of bridges, and recommends using their B3 model [17]. Unlike CEB-FIP, the B3 model considers the flow compliance of the material, whose effect persists even many decades after construction.

A realistic mechanical model of Colle Isarco viaduct is critical not only to explain its abnormal past deflection, but also to predict its future behavior, to judge the effectiveness of the new retrofit works and to provide support for future decisions on maintenance, repair and reconstruction actions [18]. To this end, Bazant's B3 constitutive law was implemented in two separate finite element (FE) models. The first is a simple statically determinate beam-like model, developed in Matlab, used to perform rapid analyses in order to capture the overall behavior of the bridge and to identify the creep model parameters. The second is a more refined 3D FE model, developed with ANSYS, used to validate the outcomes of the simpered beam model and to better estimate the values of local stresses.

3.2 1D FE Model

This is a simplified model, developed in Matlab, which reproduces the box-girder cantilever in 33 beam elements. The elastic behavior is simply reproduced with classical Euler-Bernoulli beam theory, while the two slabs are assumed to contract separately under creep and shrinkage effects, using the Bazant B3 model. The post-tensioning is modeled with two equivalent forces applied, section by section, at the centroid of the top and bottom slabs.

The prestress and external load history considers all construction phases and major maintenance works. The model simulates the segmental construction procedure, reproducing the actual static scheme realized at the different construction stages. The model also takes into account the changes in cross-section geometry following the 2014 intervention. Similarly, it accounts for the different mechanical and rheological properties of the new and old concrete, assuming perfect adherence between the old section and the new concrete layer. Because the structure is statically determinate, the effect of creep and shrinkage on the curvature is calculated separately section by section. The deflection of the bridge is then calculated using the principle of virtual work.

We calibrated the five B3 model parameters by fitting the experimental response of the bridge with the model response, using a Bayesian identification algorithm [19,20]. The prior information on the parameters was based on the design information of concrete class and mix design, consistently with [17]. Similarly, the prior uncertainty of each parameter was chosen to reproduce the variability of parameters suggested in [17].

The continuous line in Figure 3 shows that the time-deflection profile obtained by using the simplified 1D model very satisfactorily matches the observed values of deflection. The model also captures in essence all the variations in deflection that the viaduct has experienced during the past and ongoing maintenance work. For instance, the model correctly reproduces the recovery in deflection of 7 cm following the 1989 intervention.

3.3 3D FE Model

The 3D FE model was developed in ANSYS v. 12.1. The concrete structure of the bridge was implemented using SOLID186 elements, whereas the 414 cables were modeled with

8059 BEAM188 Timoshenko beam elements. The model includes a total of 260000 degrees of freedom. Each cable was placed into the model at its proper longitudinal and transversal position. Creep Model B3 was implemented in the form of a user-defined element using FORTRAN code. Friction losses in prestress were simulated by applying an equivalent thermal gradient between the two edges of each cable. The model accounts for all variation in load, geometry and boundary conditions exactly as in the simplified 1D model. The 3D model was primarily used for validating the 1D. The 3D model was used to evaluate the extent of local stresses, particularly at the anchorage blocks of the posttensioning systems.

4 MONITORING SYSTEM

The monitoring system consists of two separate parts based on different technologies. The first, installed and activated before the 2014 retrofit intervention, is made up of two topographic total stations and a set of prisms. The second part of the system, to be installed by the end of 2016, will have fiber optic sensors (FOSs) [21–25] and thermometers [26]. The topographic system was designed to monitor the deflection of the decks between pier #7 and #10 during the structural intervention and afterwards. The selected total stations are two Leica Nova TM50. Each station was installed on a 1.50 m-high concrete pile and protected by low-iron glass, which minimizes the measurement error due to refraction. The location of the two stations was chosen to ensure stability and low measurement noise, which, in general, is minimized by placing the measurement points and the benchmarks at approximately the same distance from the corresponding station and at the same altitude. GPR112 prisms were used for the 60 measurement points as well as for the 12 benchmarks, as depicted in Fig. 4. To ensure a measurement uncertainty of less than 5 mm, 6 benchmarks were used for each total station and were positioned in sparse locations around the Isarco Valley.

The system based on FOSs and PT100 [27] sensors was designed to monitor the long-term effects of the recent post-tensioning intervention. This system will record the strain measurements of the top and bottom slab of the box girders. The final design of the system consists of 48 two-meter-long thermally compensated fiber Bragg grating (FBG) sensors [28,29] and 8 one-meter-long thermally compensated fiber Bragg grating (FBG) sensors, both for the uniaxial measurement of local strain, and 80 PT100 platinum resistance thermometers for the measurement of the local concrete temperature. Each instrumented section will contain 4 FOSs—2 for each deck—while 4 acquisition units will be located near pier #8 and #9. In total, 14 sections will be measured using the FOSs. The temperature field will be measured in 10 sections: 16 PT100 sensors—8 for each deck—are designated for sections C5 and C7 (Fig. 4), while 6 PT100 sensors are designated for each of the other sections—3 for each deck. The idea is to accurately measure the temperature pattern [30] in section C5 and C7, and then obtain the pattern in the other sections using the temperatures provided by the 3 sensors as boundary conditions. Since the units that will record data from the PT100 sensors can acquire measurements from 4 different sensors at most, 4 acquisition units have to be installed in section C5 and C7, respectively, and 2—one for each deck—in the others. Figure 5 shows the sensor configuration.

The topographic monitoring system started acquiring on June 9, 2014. Fig. 6 shows the vertical displacement of prism 8N1N and 8N1S, along with the air temperature, recorded from August 4 to 9, 2014. These prisms are placed at the edge of the north girders, a location that is sensitive to variations in loads and mechanical properties. By observing these measurements, we can conclude that the behavior of the two decks before the recent post-tensioning intervention was similar and mostly affected by temperature rather than live loads.

Based on Figure 6, we can also say that when the air temperature increases in the morning the edge of each deck moves down, with a small time delay. This effect is because the source of heat—the Sun—increases the temperature of the top slab more than the bottom one, leading the top slab to elongate more than the bottom slab. In Figure 7, we show the instant effects due to post-tensioning. The figure displays one measurement per day, acquired from 5 AM to 7 AM. Three things can be observed in Fig. 7:

1) from July 31 to August 11, 2014, part of the top slab belonging to the girder bearing the southbound carriageway was removed and new concrete was cast to the required thickness; this weakened the corresponding deck, leading it to behave differently from the girder bearing the northbound carriageway;
2) from November 25 to December 3, 2014, the external cables installed in the girder bearing the southbound carriageway were tensioned causing the same deck to rise byabout 70 mm;
3) the behavior of the deck post-tensioned in 2014 is different from the other, as its deflection clearly increased more over time than that of the northbound carriageway.

In addition to what is mentioned above, Fig. 7 also shows the influence of environmental temperature. Whereas the measurements of Fig. 6 are severely influenced by the hourly effects of the Sun, which heats the top slab more than the bottom one and therefore causes the edge of the cantilever to lower, the deflection displayed by Fig. 7 seems to increase with the temperature. The reason for this is that the measurements shown by Fig. 7 were recorded before sunrise, when the temperature of the two slabs should be about the same and close to the average temperature of the air in the early morning. Based on this reasonable assumption, a global increase of the structure temperature increases the size of the whole viaduct—in particular of the piers—resulting in larger measurements of the edge deflection.

To sum up, Figure 6 shows that the uncertainty predicted during design was correct. Figure 7 shows that the effect of every stage of the 2014 intervention could be monitored with satisfactory precision, while the provided measurements can be explained by engineering judgement and structural mechanics.

6 CONCLUSIONS

Colle Isarco viaduct is one of the most critical structures in southern Europe. Erected in 1970, its main span has undergone a number of retrofit interventions aimed at controlling its abnormal deflection, preventing its deterioration, enhancing its load-carrying capacity and extending its lifespan. To predict its future behavior, to judge the effectiveness of the new retrofit works and to provide support for future decisions on maintenance and repair, it is essential to rely on (1) a reliable mechanical model of the bridge and (2) continuous monitoring of its structural response. In the case of Colle Isarco, analyses carried out using classical creep models have failed to explain its past abnormal response, while even a simple beam-like finite element model incorporating Bazant's B3 constitutive law provides very satisfactory results. The monitoring systems include two separate networks. The first, already operating, tracks the bridge deflection profile over time with an automatic topographic network. The second will shed light on the actual strain field of the box-girder cantilevers through high accuracy fiber-optic strain gauges. Monitoring will allow better assessment of future bridge performance, and a deeper comprehension of the rheological mechanisms.

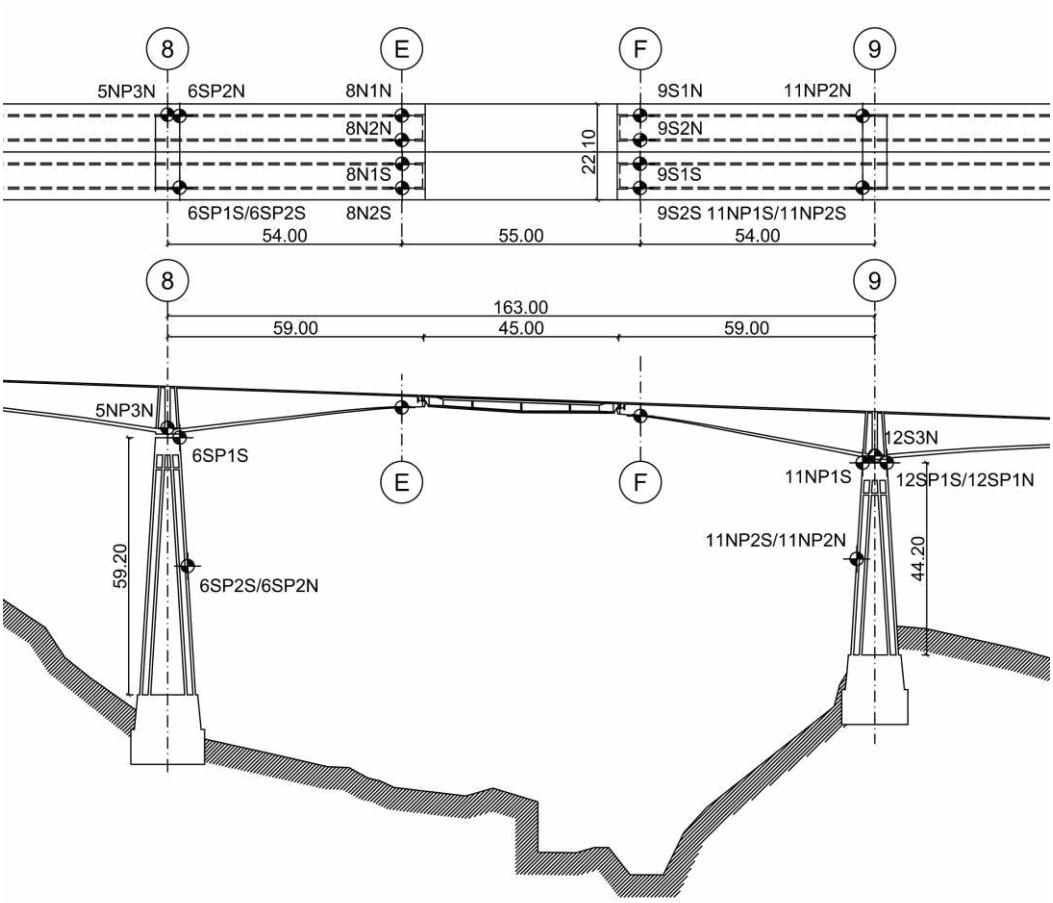

Figure 4: Prisms on piles #7 and #8, and on the north girders.

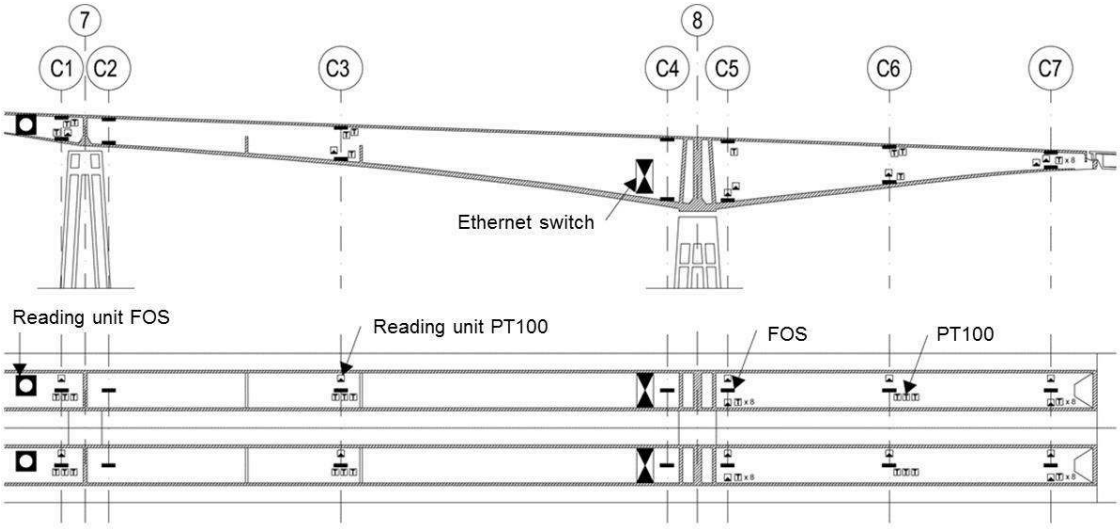

Figure 5: Configuration of fiber optic sensors (FOSs) and PT100 sensors.

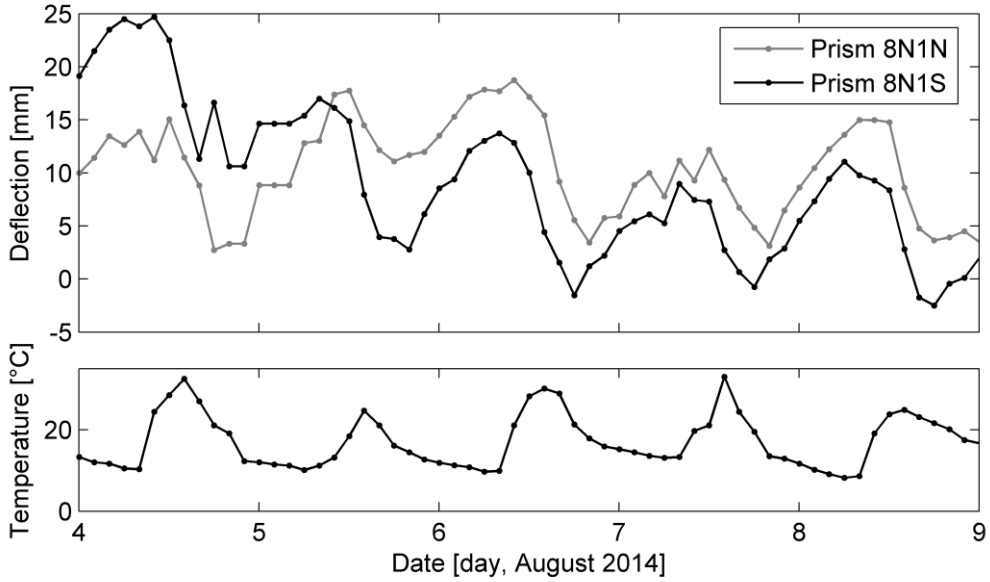

Figure 6: Deflection measured at prisms 8N1N and 8N2S; air temperature measurement; vertical black bars indicate major intervention stages

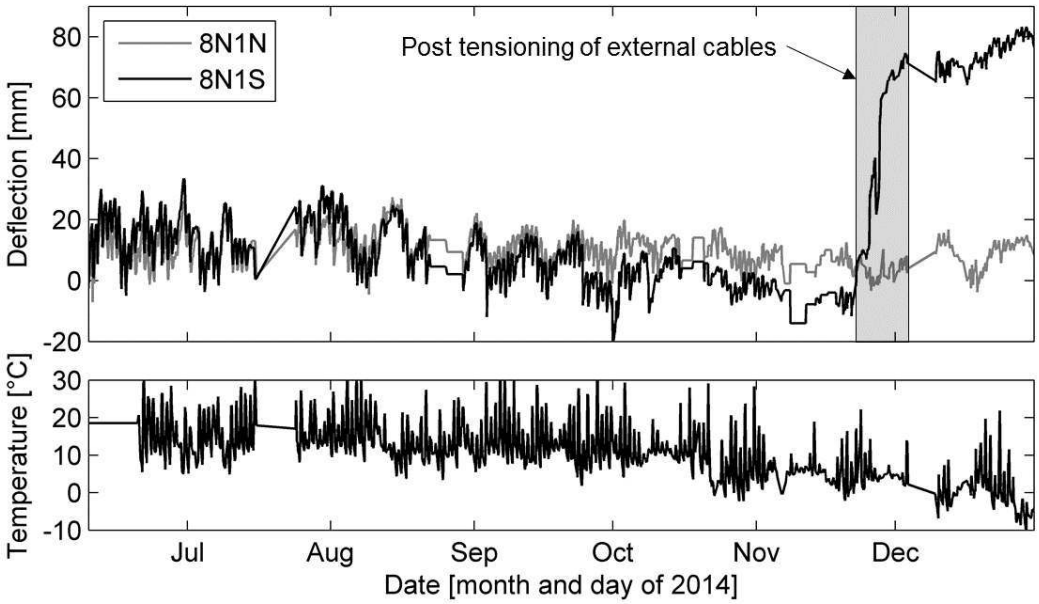

Figure 7: Deflection measured at prisms 8N1N and 8N1S; air temperature measurements; vertical black bars indicate major intervention stages

6 ACKNOWLEDGMENTS

The work presented in this paper was carried out under the research agreement between Autostrada del Brennero SpA/Brennerautobahn AG and the University of Trento. The contribution of Autostrada del Brennero is acknowledged. The authors also wish to thank all those who contributed to this project, in particular M. Fumanelli, P. Joris, S. Vivaldelli, A. Cassani, P. Mori, F. Marcato, S. Ranzi (Autostrada del Brennero SpA); M. Vivaldi (SEICO SRL); A. Massarotto, L. Mazzi, D. Trapani, A. Vallarini, S. Versini (University of Trento).

REFERENCES

[1] D. Zonta, B. Glisic, S. Adriaenssens, Value of information: impact of monitoring on decision-making. Structural Control and Health Monitoring **21**, 1043–1056, 2014.

[2] F. Bruschetta, D. Zonta, C. Cappello, R. Zandonini, M. Pozzi, B. Glisic, D. Inaudi, D. Posenato, M.-L. Wang, Y. Zhao, Bayesian analysis of monitoring data from cable-stayed bridge. Safety, Reliability, Risk and Life-Cycle Performance of Structures and Infrastructures - Proceedings of the 11th International Conference on Structural Safety and Reliability, ICOSSAR 2013, 2465–2470, 2013.

[3] D. Bolognani, D. Zonta, C. Cappello, Mechanical equivalent of logical inference: Application to monitoring data analysis. IEEE Workshop on Environmental, Energy, and Structural Monitoring Systems, EESMS 2015, 17–22, 2015.

[4] B. Glisic, D. Inaudi, Development of method for in-service crack detection based on distributed fiber optic sensors. Structural Health Monitoring, **11**, 161–171, 2012.

[5] N. Tondini, O. S. Bursi, A. Bonelli, M. Fassin, Capabilities of a Fiber Bragg Grating sensor system to monitor the inelastic response of concrete sections in new tunnel linings subjected to earthquake loading. Computer-Aided Civil and Infrastructure Engineering, **30**, 636–653, 2015.

[6] D. Zonta, A. Lanaro, P. Zanon, A strain-flexibility-based approach to damage location. Key Engineering Materials, **245**, 87–94, 2003.

[7] M. Pozzi, D. Zonta, W. Wang, G. Chen, A framework for evaluating the impact of structural health monitoring on bridge management. Bridge Maintenance, Safety, Management and Life-Cycle Optimization: Proceedings of the Fifth International IABMAS Conference, 2010.

[8] C. Cappello, R. Zandonini, D. Zonta, An implementation of expected utility theory in a civil engineering decision problema. IABSE Conference, Geneva 2015: Structural Engineering: Providing Solutions to Global Challenges, 953–960, 2015.

[9] C. Cappello, D. Zonta, B. Glisic, Expected utility theory for monitoring-based decision making. Proceedings of the IEEE. In press, 2016.

[10] B. Glisic, D. Inaudi. Fiber Optic Methods for Structural Health Monitoring. John Wiley & Sons ISBN: 9780470061428 (2007).

[11] P. A. Calderón, B. Glisic, Influence of mechanical and geometrical properties of embedded long-gauge strain sensors on the accuracy of strain measurement. Measurement Science and Technology, **23**, 2012.

[12] D. Inaudi, B. Glisic, Integration of distributed strain and temperature sensors in composite coiled tubing. Proceedings of SPIE - The International Society for Optical Engineering 6167, 2006.

[13] S. Erlicher, O. S. Bursi, Bouc-Wen-type models with stiffness degradation: Thermodynamic analysis and applications. Journal of Engineering Mechanics – ASCE, **134**, 843–855, 2008.

[14] B. Gentilini, L. Gentilini, Il viadotto di Colle Isarco per l'Autostrada del Brennero. *L'Industria Italiana del Cemento*, **5**, 318–334, 1972.

[15] Autostrada del Brennero SpA. *Consolidamento strutturale dell'impalcato del viadotto* colle isarco, a progressiva km 8+957. Perizia di variante. Technical report (2013).

[16] CEB (Comité Euro-International du Béton). CEB-FIP model code 1990. Thomas Telford Ltd (2008).

[17] Z. P. Bazant, S. Baweja, Creep and shrinkage prediction model for analysis and design of concrete structures – model B3. Materials and Structures, **28**, 357–365, 1995.

[18] O.S. Bursi, M. T. Vannan, Pseudodynamic tests of a concentrically braced frame using substructuring techniques. Journal of Contructional Steel Research, **29**, 121–148, 1994.

[19] W. M. Bolstad. Understanding Computational Bayesian Statistics. Wiley ISBN: 9780470046098 (2010).

[20] C. Cappello, D. Zonta, M. Pozzi, R. Zandonini, Impact of prior perception on bridge health diagnosis. Journal of Civil Structural Health Monitoring, **5**, 509–525, 2015.

[21] B. Glisic, D. Inaudi, Long-gage fiber optic sensors for global structural monitoring. The First International Workshop on Structural Health Monitoring of Innovative Civil Engineering Structures, 2002.

[22] B. Glisic, D. Inaudi, Integration of long-gage fiber-optic sensor into a fiber-reinforced composite sensing tape. Proceedings of SPIE – The International Society for Optical Engineering 5050, 179–186, 2003.

[23] D. Zonta, A. Chiappini, A. Chiasera, M. Ferrari, M. Pozzi, L. Battisti, M. Benedetti, Photonic crystals for monitoring fatigue phenomena in steel structures. Proceedings of SPIE - The International Society for Optical Engineering, **7292**, 2009.

[24] B. Glisic, Influence of the gauge length on the accuracy of long-gauge sensors employed in monitoring of prismatic beams. Measurement Science and Technology, **22**, 2011.

[25] M. Pozzi, D. Zonta, H. Wu, D. Inaudi, Development and laboratory validation of in-line multiplexed low-coherence interferometric sensors. Optical Fiber Technology, **14**, 281–293, 2008.

[26] M. Enckell, B. Glisic, F. Myrvoll, B. Bergstrand, Evaluation of a large-scale bridge strain, temperature and crack monitoring with distributed fibre optic sensors. Journal of Civil Structural Health Monitoring, **1**, 37-46, 2011.

[27] F. Bruschetta, D. Zonta, C. Cappello, R. Zandonini, M. Pozzi, B. Glisic, D. Inaudi, D. Posenato, M.-L. Wang, Y. Zhao, Fusion of monitoring data from cable-stayed bridge. IEEE Workshop on Environmental, Energy and Structural Monitoring Systems, EESMS 2013, 2013.

[28] B. Glisic, D. Inaudi, C. Nan, Pile monitoring with fiber optic sensors during axial compression, pullout, and flexure tests. Transportation Research Record (1808), 11–20, 2002.

[29] D. H. Sigurdardottir, B. Glisic, Neutral axis as damage sensitive feature. Smart Materials and Structures, **22**, 2013.

[30] D. Zonta, C. Modena, Observations on the appearance of dispersive phenomena in damaged structures. Journal of Sound and Vibration, **241**, 925–933, 2001.